Pacific Northwest
NATIONAL LABORATORY

PNNL-32268

Surface Acoustic Wave Sensors for Refrigerant Leak Detection

Compact, Inexpensive, Selective and Sensitive Sensors

October 2021

Praveen K. Thallapally (PNNL)
Jian Liu (PNNL)
Huidong Li (PNNL)
Jun Lu (PNNL)
Jay W Grate (PNNL)
Peter B McGrail (PNNL)
Daniel Deng (PNNL)
Fitria Fnu (Washington State University, WSU)

Raghu Kunapuli (Parker and Hannifin)
Debasis Banerjee (Parker and Hannifin)
Max A. Witter (Parker and Hannifin)

U.S. DEPARTMENT OF ENERGY

Prepared for the U.S. Department of Energy
under Contract DE-AC05-76RL01830

DISCLAIMER

PACIFIC NORTHWEST NATIONAL LABORATORY
operated by
BATTELLE
for the
UNITED STATES DEPARTMENT OF ENERGY
under Contract DE-AC05-76RL01830

Printed in the United States of America

Available to DOE and DOE contractors from the
Office of Scientific and Technical Information,
P.O. Box 62, Oak Ridge, TN 37831-0062;
ph: (865) 576-8401
fax: (865) 576-5728
email: reports@adonis.osti.gov

Available to the public from the National Technical Information Service
5301 Shawnee Rd., Alexandria, VA 22312
ph: (800) 553-NTIS (6847)
email: orders@ntis.gov <https://www.ntis.gov/about>
Online ordering: http://www.ntis.gov

PNNL-32268

Surface Acoustic Wave Sensors for Refrigerant Leak Detection

Compact, Inexpensive, Selective and Sensitive Sensors

October 2021

Praveen K. Thallapally (PNNL)
Jian Liu (PNNL)
Huidong Li (PNNL)
Jun Lu (PNNL)
Jay W Grate (PNNL)
Peter B McGrail (PNNL)
Daniel Deng (PNNL)
Fitria Fnu (Washington State University, WSU)

Raghu Kunapuli (Parker and Hannifin)
Debasis Banerjee (Parker and Hannifin)
Max A. Witter (Parker and Hannifin)

Prepared for
the U.S. Department of Energy
under Contract DE-AC05-76RL01830

Pacific Northwest National Laboratory
Richland, Washington 99354

Abstract

Pacific Northwest National Laboratory (PNNL), in collaboration with Parker and Hannifin, is developing a compact, inexpensive, and highly sensitive and selective surface acoustic wave sensor coated with fluorophillic sorbent for detecting fluorocarbon leaks from HVAC systems. Having a highly effective sorbent sensitive to fluorocarbon refrigerant vapors provides a means to develop a sensing device for leak detection. Surface acoustic wave (SAW) sensors with a gas sensing film deposited between the delay lines or on the interdigital transducer have been used to detect gas and vapor molecules in harsh environments with high sensitivity. As part of this project, PNNL screened several sorbent materials that are shown to be selective towards fluorocarbon refrigerant (R32) molecule. The identified sorbent materials were synthesized, characterized, and tested towards R32 using various spectroscopic techniques. Next, the sorbent material was coated on a SAW sensor as a thin film using vapor deposition and drop coating methods. The coated thin film was further characterized and tested towards the detection of pure R32 and R32 in ambient air at room temperature to demonstrate the SAW response towards R32 in presence of other competing gases and vapors in air.

This report completes the milestone 2.1entitled Demonstrate SAW sensor detection limit performance in pure vapor at 36,000 to 100 ppmv and 2.2 entitled Demonstrate SAW sensor detection capability for R32 at 36,000 ppmv or less in air.

Summary

Pacific Northwest National Laboratory (PNNL), in collaboration with Parker and Hannifin, developed a compact, inexpensive, and highly sensitive and selective surface acoustic wave sensor coated with fluorophillic sorbent for detecting fluorocarbon leaks from HVAC systems. Having a highly effective sorbent sensitive to fluorocarbon refrigerant vapors provides a means to develop a sensing device for leak detection. Surface acoustic wave (SAW) sensors with a gas sensing film deposited between the delay lines or on the interdigital transducer have been used to detect gas and vapor molecules in harsh environments with high sensitivity. As part of this project, PNNL screened several sorbent materials that are shown to be selective towards fluorocarbon refrigerant (R32) molecule. The identified sorbent materials were synthesized, characterized, and tested towards R32 using various spectroscopic techniques. Next, the sorbent material was coated on a SAW sensor as a thin film using vapor deposition and drop coating methods. The coated thin film was further characterized and tested towards the detection of pure R32 and R32 in ambient air at room temperature to demonstrate the SAW response towards R32 in presence of other competing gases and vapors in ambient air.

Acknowledgments

We thank DOE Building Technology Office (BTO) Program for funding particularly, Dr. Tony Bouza program manager at BTO for his support. We also thank Dr. Denis Stiles and Dr. Bing Liu for support and encouragement during this project.

Acronyms and Abbreviations

CSPH	Conductive Supramolecular Polymer Hydrogel
HVAC&R	Heating Ventilation Air Conditioning and Refrigeration
IDT	Inter Digital Transducer
LFL	Lower Flammable Limit
MOF	Metal Organic Framework
MIL-101	Material of Institute Lavoisier-101
PXRD	Powder X-ray Diffraction
PVB	Polyvinyl Butyral
QCM	Quartz Crystal Microbalance
R32	Difluoromethane
SAW	Surface Acoustic Wave Sensor
TBC4	Tert-butyl[4]calixarene

Contents

Figures

1.0 Introduction

When a refrigerant leak occurs from an HVAC&R system, there are several direct and indirect consequences that include reduction in cooling efficiency and higher CO_2 emissions. The reduction in colling efficiency results in increased power consumption and costs for the additional kWh consumed until the leak is detected and repaired.[1] Further, depending on the global warming potential of the refrigerant additional greenhouse gas emissions to the atmosphere. When considering flammable A2L or A3 refrigerants, refrigerant leaks take on an additional overriding consideration regarding the safety of the occupants in the building. Reliable detection of refrigerant leaks is thus a critical technology necessary to enable more widespread use of class A2L and A3 refrigerants in HVAC&R systems. Several existing methods have been developed for refrigerant leak detection that includes optical, electrical, and olfactory methods.[2] Standard optical methods include adding a fluorescent dye into the refrigerant that becomes visible under laser or UV light or monitoring IR absorption with a hand-held unit.[3] Electrical methods typically involve an electrical or coronal discharge across electrodes with the electrical conductivity of the sensing electrode varying in response to refrigerant concentration. Olfactory methods involve the addition of mercaptans, ammonia, or other odorous compounds that can be detected by smell. All of these methods have been designed for detecting leaks when an HVAC&R system is being serviced. They are not autonomous systems that can detect and alert the building owner when a leak occurs under normal unattended operating conditions. Moreover, these sensing methods and enabling detection devices were found to be cost-prohibitive for an integrated sensing system designed as part of the HVAC&R unit.

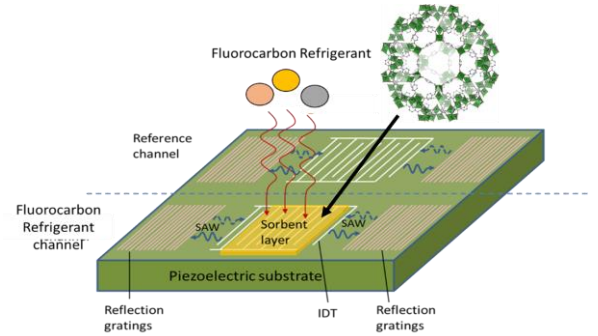

Figure 1. SAW sensor platform with a selective sorbent

Similarly, spectroscopic methods are available including surface plasmon resonance spectroscopy, FTIR, and NMR techniques, but none of these are suitable for a low cost sensor application. However, the change in mass that occurs from the adsorption of gas can, in theory, provide a very sensitive means to detect refrigerant leaks with the proper adsorbent. For example, the quartz crystal microbalance method is sensitive to ng-level changes in mass of the oscillating crystal.[4] Even higher sensitivity to mass change is possible with a similar method based on propagation of surface acoustic waves. Surface acoustic waves are typically generated by exciting an interdigital transducer (IDT) deposited on a piezoelectric substrate. As an AC signal is applied to the IDT, a SAW is generated and propagated through the substrate and be detected by another IDT, which converts the mechanical signal back to an alternating electrical signal due to the direct piezoelectric effect. By placing a sensing thin film along the SAW's propagation path, a frequency or phase shift can be observed through the receiving IDT due to surface perturbation, thus providing a sensing output (**Figure 1**). SAW sensors have been used to detect various gases and vapors under harsh environments with high sensitivity however never been explored nor used for the detection of refrigerant leaks.[5-8] Therefore, as part of this project we identified a sorbent that is selective to fluorocarbon refrigerant particularly difluoromethane (R32), fabricated the sorbent into gas sensing film on a SAW using vapor deposition and/or drop coating approaches and demonstrated the performance of the SAW towards refrigerant leak detention with and without competing gases and vapors by measuring the phase shift.

2.0 Sorbent Selection and Characterization

As detailed in the previous quarterly report, several candidate materials were selected based on commercial availability, easy synthesis, pore size, hydrophobicity, and thin film fabrication. Based on the literature data and our work in this area, three carbon-based materials along with a metal organic framework (MOF) material was identified as a possible candidate for refrigerant leak detection.[9-11] The sorbent materials include *tert*-butylcalix[4]arene, TBC4, porous organic cage (CC3) and Ketjen black activated carbon (Obtained from Parker and Hannifin). Both TBC4 and CC3 were synthesized at a small scale using a literature procedure. [12-13] The porous form of TBC4 can be obtained by sublimation of commercially available TBC4 powder under reduced pressure at 200 C. Once obtained, difluoromethane (R32) adsorption experiments were carried out at room temperature at concentrations between 0 and 36,000 ppmv. **Figure 2** shows the R32 adsorption for three materials identified, which show high uptake at low concentration, particularly TBC4. Along with the sorbent identified here, we also tested the R32 adsorption at room temperature in activated carbon materials received from our industrial partner (**Figure 3**). To down select the sorbent for thin film fabrication, experiments were conducted on TBC4 and activated carbon materials (labeled as F400 and F600) towards CO_2, and water. **Figures 3** show the single-component CO_2, and water adsorption under identical conditions for the three sorbent materials tested. TBC4 has a much higher R32 adsorption capacity (5X), especially at concentration close to 36,000 ppm (about 0.036 bar), compared to those of the two carbon materials, F400 and F600. All three sorbents show relatively low CO_2 uptake at the concentrations found in the building, but TBC4 is shown to have much lower capacity compared to activated carbon materials, although the result is hard to quantify due to the low concentration (about 1500 ppm) of CO_2 in the buildings. Similarly, the two carbon materials, F400 and F600, show typical H_2O adsorption isotherms. Water will condense inside the pores of the two carbon materials at RH levels higher than 60%. TBC4 shows a hydrophobic behavior, and H_2O adsorption capacity stays at a low level throughout the RH range. Based on the available data on R32 uptake, selectivity over CO_2/water at lower

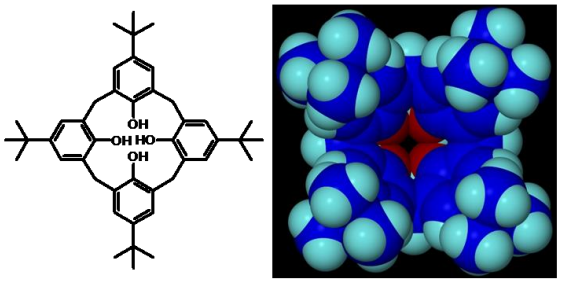

TBC4

Sublimation

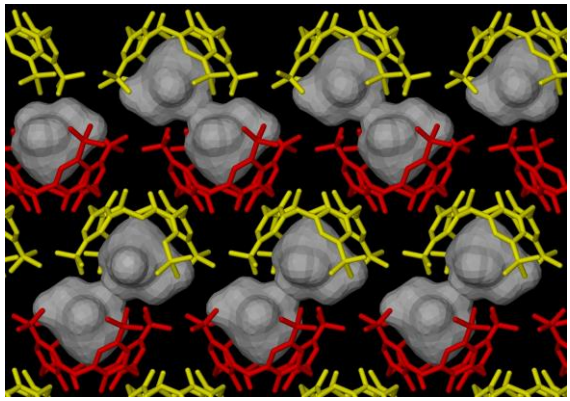

TBC4 active form

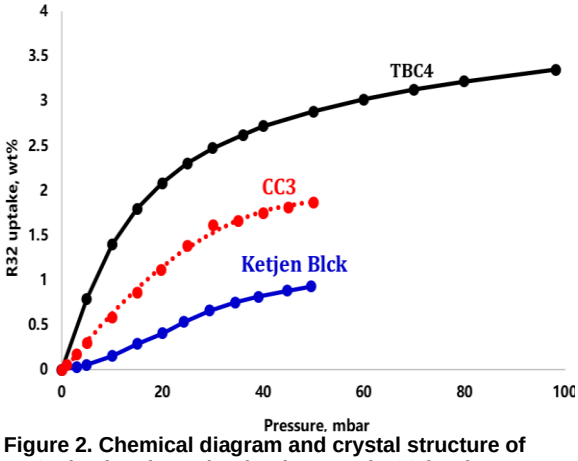

Figure 2. Chemical diagram and crystal structure of TBC4 (top). Adsorption isotherms of R32 for three adsorbent materials identified.

concentrations, and easy thin film fabrication, TBC4 was down selected as an ideal material for single-channel sensor design.

Similarly, a well-known MOF (known as MIL-101) was identified as an alternate to TBC4 due to its exceptional capacity towards R32 however this sorbent is hydrophilic and known to adsorb a significant amount of water from the air.[14] R32 and water adsorption isotherms for MIL-101 were shown in **Figure 4**. Although MIL-101 has preferential adsorption towards CO_2 and water over R32, coating the MIL-101 with hydrophobic polymer has several advantages that include reduced water and CO_2 uptake and better adhesion to the QCM substrate.[15-16] Therefore, TBC4 and MIL-101 were identified as the sensing material candidate for further study.

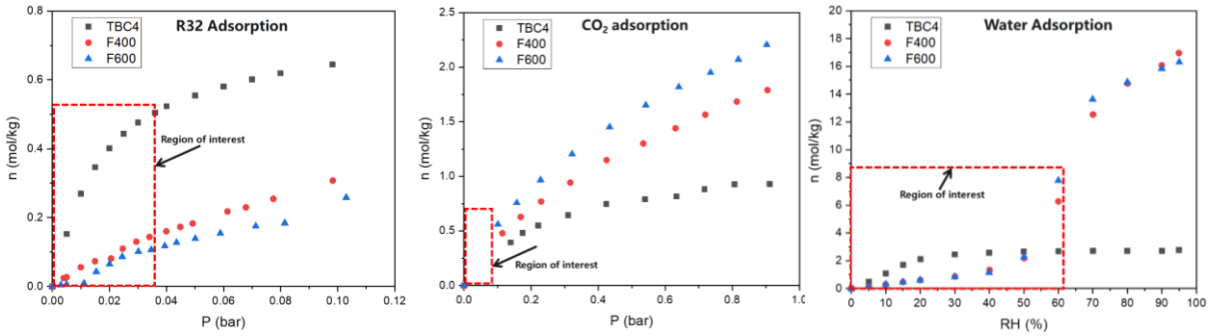

Figure 3. Adsorption isotherms of CO2 (left) and R32 for three carbon based adsorbent materials. Water adsorption in TBC4 and activated carbon materials were received from Parker

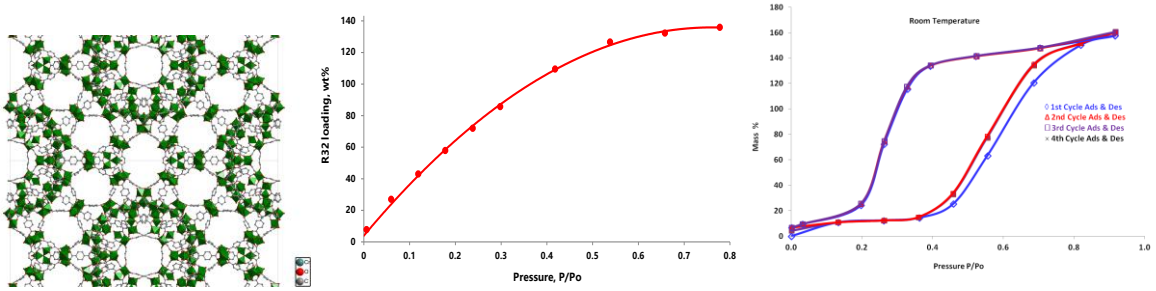

Figure 4. Crystal structure of MIL-101, R32 adsorption and water adsorption and desorption profiles at room temperature.

3.0 Thin Film Fabrication and Sensor Development

To fabricate thin film on the SAW substrate using the two sorbents identified above, we adapted the vapor deposition technique for TBC4 and the drop coating method for MIL-101. **Figure 5** shows a step-by-step process from fabricating sensor film to the evaluation of the thin film using Quartz Crystal Microbalance (QCM) and SAW platforms. QCM platform was selected to evaluate the coating methods and the response of the sensing film toward R32. A QCM sensor with a default frequency of 10 MHz was cleaned and porous TBC4 was deposited to the QCM substrate under vacuum and high temperature (~150 C) through sublimation using a homemade reactor chamber as shown in **Figure 6**. The TBC4 was placed inside of the stainless-steel tube enclosed by the heat blocks. Then, the reactor was sealed and evacuated. The TBC4 powder was heated under vacuum to deposit a thin film sprayed through a small nozzle. A decrease of about 3,700 Hz in the frequency signal was observed (**Figure 7**) while coating TBC4 film on a QCM sensor. The total time it took to deposit a TBC4 film was 60 minutes. From 0-16 min, the two QCM sensors were at room temperature with atmospheric pressure and the frequencies did not change for either sensor. When the temperature was increased to 100 °C and the pressure was decreased to 0.1 bar from 17-20 min, the frequency of the "test" QCM slightly decreased and the frequency of the "reference" QCM did not change. When the temperature was further increased to 150 °C during the 21-35 min period, the frequency change of the "test" QCM increased to about 3500 Hz and the frequency of the "reference" channel decreased by about 30 Hz. Then, the heating block was turned off and the temperature at the nozzle decreased to 24 °C (36-60 min). The frequency change of the "test" QCM sensor further increased to over 3730 Hz and the frequency change of the "reference" QCM sensor stayed at about 30 Hz. The TBC4 loadings were estimated from the mass sensitivity of the QCM sensor (4.4 ng/cm^2 Hz).[17] The mass sensitivity (k) was calculated using the relationship:

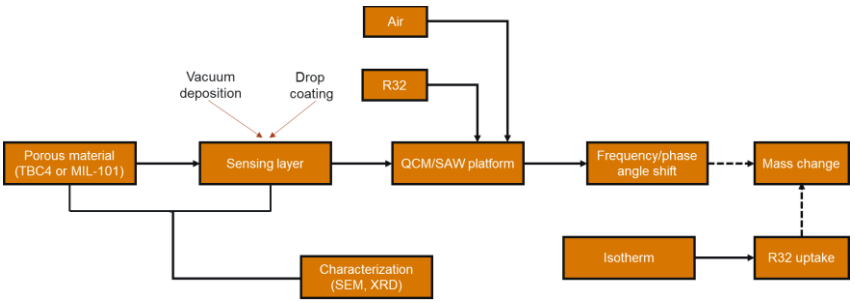

Figure 5. Flowsheet process for sensing film coating and sensor response evaluation

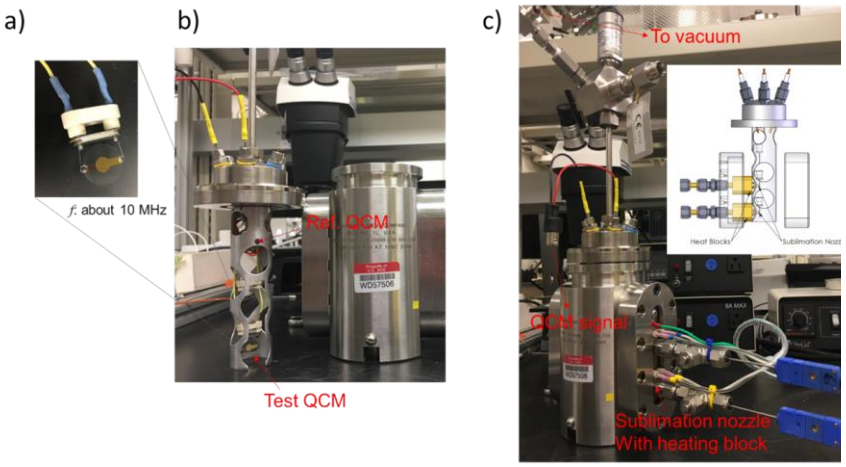

Figure 6. The sublimation system to deposit TBC4 thin film on top of the QCM sensor: a) QCM sensor, b) QCM sensor sample holder, c) heating block and

$$k = \frac{\sqrt{u_q \rho_q}}{2 f_o^2}$$

where f_o is the frequency of quartz crystal without mass loading (10 MHz), u_q is the shear modulus of AT-cut quartz cystal (2.947E11 g cm^{-1}s^{-2}), and ρ_q is the density of quartz (2.643 g cm^{-3}).

After comparing the results for the “test” and “reference” QCM sensors, we believe that the frequency change of the test QCM is clearly due to the TBC4 mass loading. The estimated mass loading of TBC4 can be calculated to be about 3200 ng by using the change of frequency times the area of the electrode (diameter 0.51 cm) and the mass sensitivity.[18] The frequency of the “test” QCM was evaluated again the next day and the reading was maintained.

Like TBC4, MIL-101 was deposited to the QCM (later SAW substrate) through drop coating as opposed to vapor deposition with a polymer binder to improve the adhesion of the MOF film. First, the QCM substrate was cleaned by acetone washing followed by plasma (5 min) cleaning. Plasma cleaning was well-known approach to clean the surface using energetic plasma created by gas species (oxygen). After plasma treatment, the MIL-101 nano-dispersant with polymer was drop cast on the QCM film. In brief, the MIL-101 nano-dispersion was prepared with a concentration of about 0.2 g/L was prepared in 5 ml methanol. Then poly(vinyl butyral) (10 wt% of MIL-101) was added to the 5 ml MIL-101 dispersion. The mixtures were then thoroughly mixed and deposited on top of QCM sensors using a micropipette. The morphologies of the deposited porous sensing layers were characterized with SEM. The TBC4 layer deposited through vacuum deposition is sparky and the particle domains are in 20-50 µm (**Figure 8**). The particle size of the MIL-101 layer deposited through drop coating is about 100-130 nm and the MIL-101 particles are somewhat more uniformly arranged compared to the TBC4 layer (**Figure 8**). The deposition rates of the sensing film for vacuum deposition and drop coating were recorded and compared in **Figure 9**. The deposition rate of TBC4 coating in the vacuum deposition process is constant at the deposition temperature (200 ºC). The deposition rate can be estimated to be about 173.7 ng TBC4/min. The deposition rate dramatically stopped after the heating was turned off which confirmed that the deposition was generated by the sublimation of TBC4 under heating and vacuum. The deposition rate of the drop coating method is not linearly related to the volume of dispersion. One possible reason is that the sublimed TBC4 particles did not disperse very well in common organic solvent including methanol so the mass of TBC4 particle in each drop (4 µl) varied which led to a different frequency change to the QCM sensor. Therefore, it is easier and more accurate to control the thickness of the TBC4 coating using the vacuum deposition method. However, it is possible to use the drop coating method to achieve the desired thickness provided that the frequency can be measured after each deposition using a micropipette.

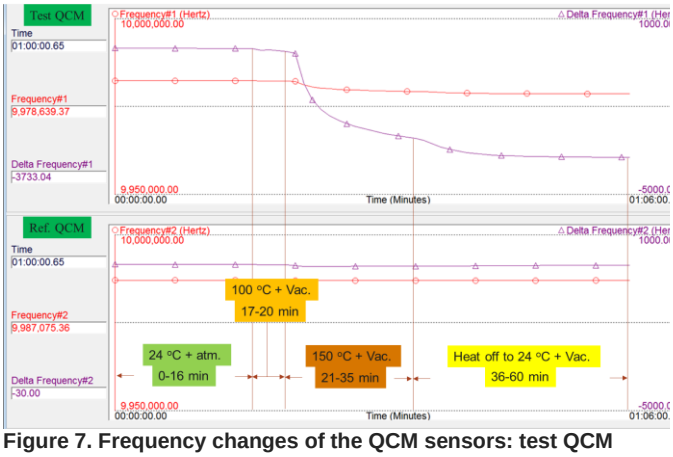

Figure 7. Frequency changes of the QCM sensors: test QCM (top), reference QCM (bottom).

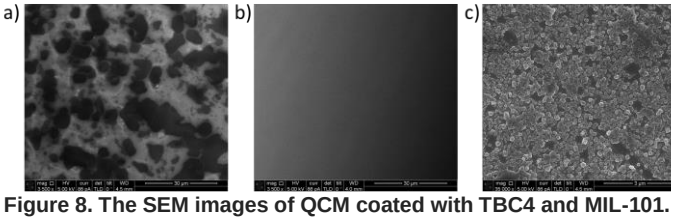

Figure 8. The SEM images of QCM coated with TBC4 and MIL-101. a) TBC4 coating obtained through vacuum deposition; b) Clean QCM substrate; c) MIL-101 coating obtained through drop coating.

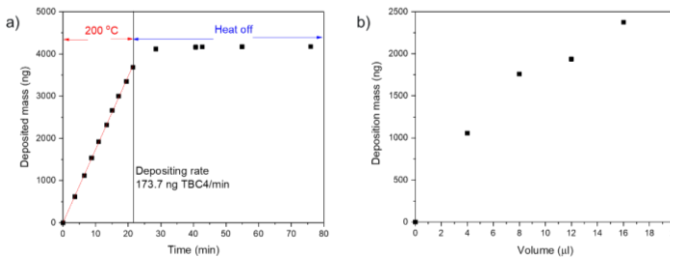

Figure 9. The deposition rate of TBC4 using different methods. a) vacuum deposition at 200 ºC; b) drop coating deposition using methanol as the dispersion solvent

3.1 QCM Sensor Performance and Testing:

The two QCM sensors loaded with TBC4 and MIL-101 were exposed to pure R32 and a mixture of R32 in dry air to test the sensing performance by recording the frequency change of the QCM sensor. The test system was evacuated overnight to remove any interferant gas from the vessel. A reference blank QCM sensor was also put inside the test chamber and its result was used as the baseline to compare with that of the coated sensor. The frequency change results for pure R32 adsorption on TBC4 were shown in **Figure 10**. Compared to the frequency change caused by only air exposure (10 Hz at about 4 psi), the QCM sensors showed a higher change of frequency (25-40 Hz at about 4 psi) toward R32 vapor. This result indicates selective adsorption of R32 over other gas components present in the air. In addition, the R32 test were repeated twice, and the results are reproducible. However, the frequency changes observed from the R32 tests for both the QCM sensors loaded with TBC4 and MIL-101 are only small portions (2-3%) of the predicted frequency changes based on the equilibrium adsorption uptakes from the isotherm data. Similar results were observed for MIL-101 as shown in **Figure 11**. Differences were observed for the QCM sensor with MIL-101 coatings compared to the reference sensor, but the frequency change is not in the same order of magnitude of the frequency change predicted from the adsorption isotherm. Several possibilities for such low frequency shift include i) film thickness, and ii) heterogeneous growth of TBC4. For applications in sensor technology, the diffusion into these layers plays a decisive role. Due to the inhomogeneity of the layers, diffusion of gas molecules into the thin film is restricted therefore uniform coating is required.

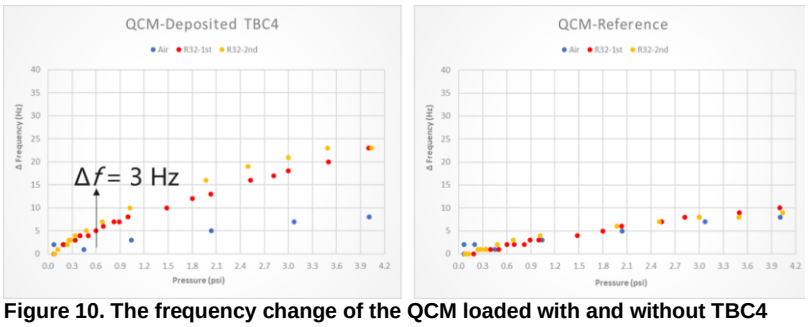

Figure 10. The frequency change of the QCM loaded with and without TBC4 coating obtained through vacuum deposition in presence of pure R32 and air. Left: experiment QCM sensor; right: reference QCM sensor.

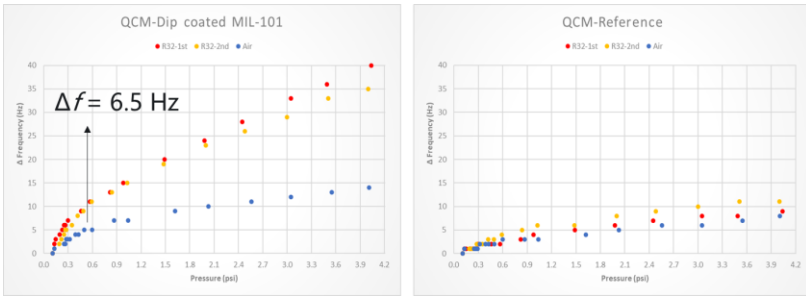

Figure 11. The frequency change of the QCM loaded with and without MIL-101 in presence of pure R32 and air. Left: experiment QCM sensor; right: reference QCM sensor.

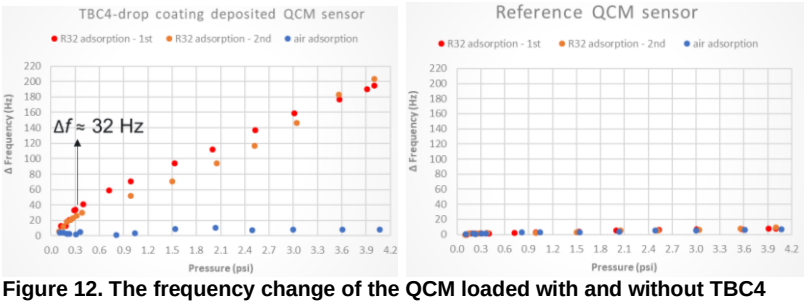

Figure 12. The frequency change of the QCM loaded with and without TBC4 coating obtained through drop coating in presence of pure R32 and air.

Therefore, experiments were conducted to coat a uniform thin film of TBC4 by dip-coating method as opposed to vapor deposition discussed above. The porous form of TBC4 was dispersed in a solution containing methanol and deposited on the QCM and evacuated overnight to remove any interferant solvent molecules from the surface of QCM. The QCM sensor loaded with TBC4 coating through drop coating was exposed to pure R32 and air at room temperature and the test results are shown in **Figure 12**. This time, the QCM sensor showed a much higher change of frequency (32 Hz at about 0.3 psi) toward R32 vapor compared to a negligible change in frequency when exposed to air at various pressures. These results indicate significant improvement from the previous test where the R32 frequency change was very minimal (3 vs 32 Hz). The frequency change for QCM sensors loaded with TBC4 is close to 40% of the predicted frequency changes based on the equilibrium adsorption uptake. Our QCM results indicated that the TBC4 coating directly on the QCM sensor did not have a frequency change that matches the predicted from the R32 adsorption isotherm in the porous TBC4 (sublimed TBC4). It seems that the TBC4 film-coated through the vacuum deposition on the QCM substrate (with the gold electrode) showed some preferred crystal orientation as shown in **Figure 13**. To avoid the preferred crystal orientation, we deposited a PVB layer and then deposited the TBC4 through vacuum deposition so that there is no induction of crystal growth from the substrate. The TBC4@PVB was tested again with pure R32 vapor and results were compared with those of the TBC4 coating obtained through drop coating in **Figure 14**. TBC4@PVB indicates that the TBC4 coating was obtained on top of a PVB layer through vacuum deposition. TBC4 indicates that the coating was obtained through drop coating. The highest frequency change for the TBC4@PVB sample matched 97.8% of the theoretical value estimated from the isotherm data. This signal dropped to 48.9% in the second run, and it seems that the signal maintained at around 48% in the third run. So adding a layer of amorphous PVB did help the growth of porous TBC4 which would lead to a higher adsorption affinity toward R32 as indicated from the significantly increased frequency changes of the TBC4@PVB sample.

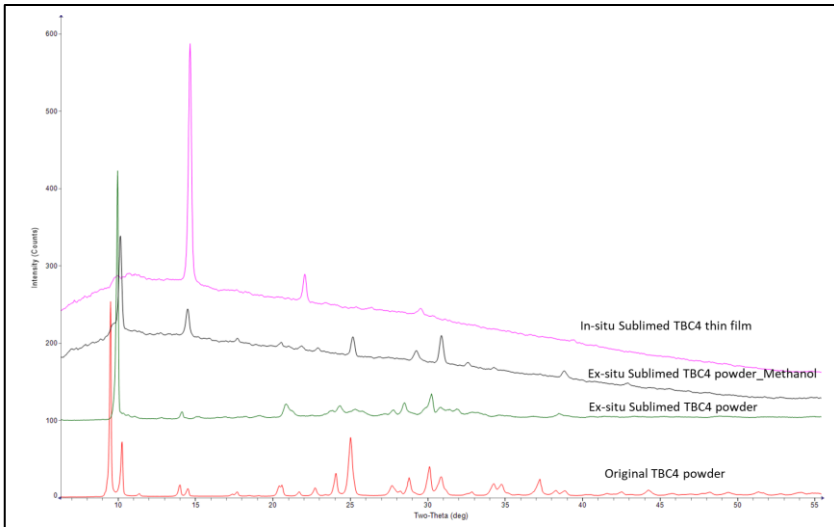

Figure 13. The XRD pattern of TBC4 powder, sublimed and thin film

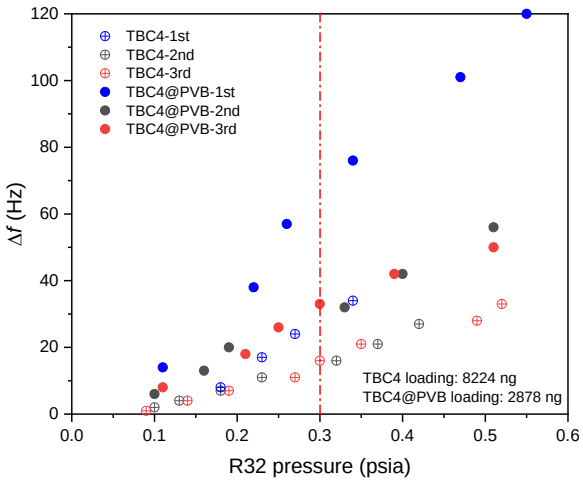

Figure 14 Frequency change for QCM sensor toward pure R32 with different TBC4 coatings.

3.2 SAW Sensor Performance and Testing:

Given the successful deposition of TBC4 and MIL-101 on a QCM sensor and its response towards R32, next, we extended our fabrication process to deposit a thin layer of TBC4 and MIL-101 on a commercially available Love-wave (LW) SAW sensor obtained from AW sensors and modified with mass flow controller (MFC) to deliver R32 and dry air into the flow cell through a 1/16-inch tube. The length of the tube connecting the mixing tee and the flow cell was minimized to less than 1/2 inch to minimize the signal delay. The SAW sensor uses a phase-shift configuration. It determines the concentration of R32 by measuring the phase difference between the input signal and output signal. **Figure 15** is an example of the circuit configuration for the SAW sensor. As R32 gets absorbed by the sorbent film deposited on the SAW sensor, the phase velocity of the acoustic wave propagating in the SAW sensor changes and thus causes a phase shift in the output signal. The sensing circuit compares the output signal of the sensor to the reference signal, which is the input signal, to obtain the phase shift. As the extent of the phase shift scales with the amount of the R32 absorbed, the concentration of R32 in the gas sample can be determined.

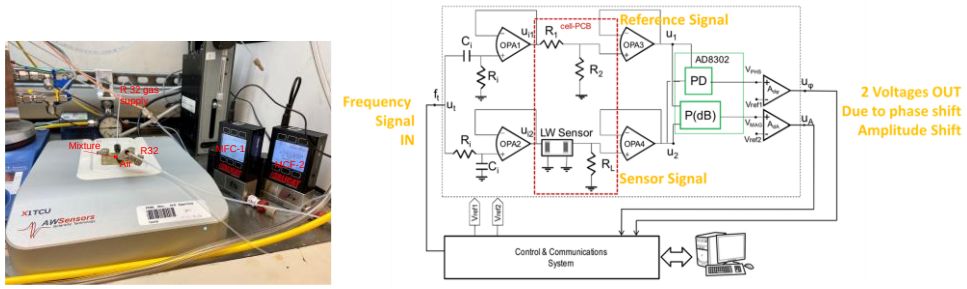

Figure 15. The SAW sensor platform used to evaluate the sensing toward the detection of R32 mixture in air

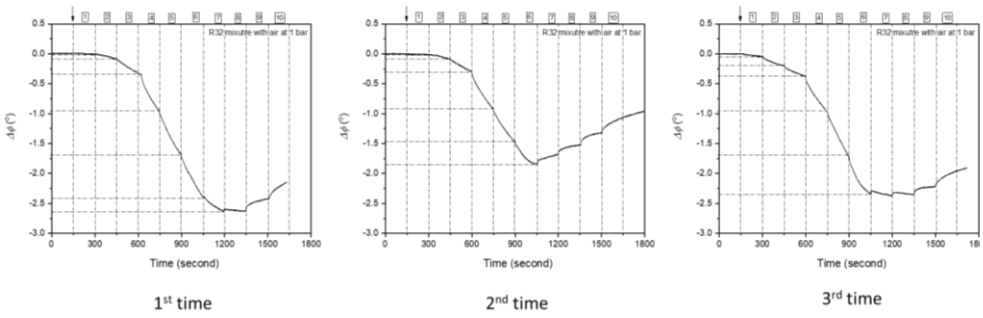

Figure 16. Comparison of SAW sensor test result for the TBC4 coating on top of PVB layer.

Each experiment with the SAW sensor was conducted three times, first SAW experiment is right after the sorbent coating, the second experiment after purging the sensor with dry air without heating, the third experiment after a brief regeneration under vacuum and 120 ^{o}C. The first sample we tested using our SAW platform is TBC4 directly deposited on top of a SAW substrate using vapor deposition technique and the phase change in response to R32 adsorption is shown in **Figure 16**. The sensor was put under dry air for 30 min with a flow rate of 20 standard cubic centimeters (sccm) before the test and then the flow rate combination of air and R32 was set to 20 sccm and 0.1 sccm (R32 concentration ~5,000 ppm), 20 sccm and 0.5 sccm (R32 concentration ~25,000 ppm), 20 sccm and 1 sccm (R32 concentration ~50,000 ppm), 15 sccm and 5 sccm (R32 concentration ~250,000 ppm), 10 sccm and 10 sccm (R32 concentration ~500,000 ppm), 0 sccm and 20 sccm (Pure R32). After the SAW sensor was exposed to the pure R32, desorption of R32 was conducted by flowing the SAW sensor with dry air. The time interval between each step is shown as the x-axis and the change of phase shift is shown as the y-axis. As shown in **Figure 16**, the TBC4 coated SAW response or phase shift started to decrease when performed

the three times. In the first experiment the phase shift was very clear with R32 in presence of air. After the first experiment the TBC4 coated SAW sensor was recycled by flowing with dry air without heating, assuming R32 will be desorbed completely from the TBC4 film however as shown in **Figure 16 (middle)** the reduced phase shift with R32 in air was observed. This could be due to the incomplete activation of the R32 from TBC4 film under flowing air. To test this hypothesis, SAW sensor coated with TBC4 film was activated for 15 min under vacuum at 120 ^{o}C. After cooling the SAW senor to room temperature, the experiments were conducted with same composition as described earlier. As shown in Figure 16(left), the SAW sensor coated with TBC4 regained the phase shift.

Similar sensor response was recorded using TBC4 mixed with 10% PVB polymer drop cast onto the SAW sensor as opposed to vapor deposition. The SAW response or phase shift was recorded with R32 and air mixture at room temperature and the results are shown in **Figure 17**. As shown in **Figure 17** left, the SAW sensor drop coated with TBC4/PVB showed a smaller phase shift compared to the SAW sensor vacuum-deposited with TBC4 on top of the PVB layer **(Figure 16)**. After the experiment, the SAW film was regenerated by flowing dry air through the SAW film and sensor response was recorded by flowing R32 and air mixture. As shown in **Figure 17,** the drop-coated sensor also showed decreased phase shift as expected due to incomplete activation of the TBC4. However, SAW sensor performance (phase shift) did not revert to the original phase shift even after brief heating **(Figure 17 (right))**. Further experiments are needed to evaluate the optimal temperature to revert to the original phase shift.

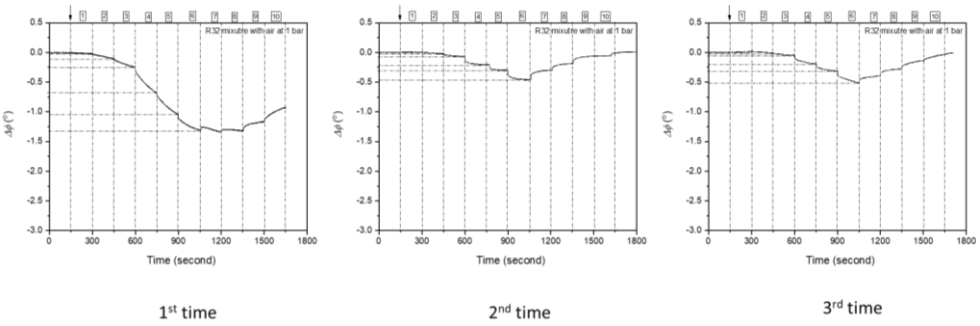

Figure 17. Comparison of SAW sensor test result for the TBC4/PVB drop coating.

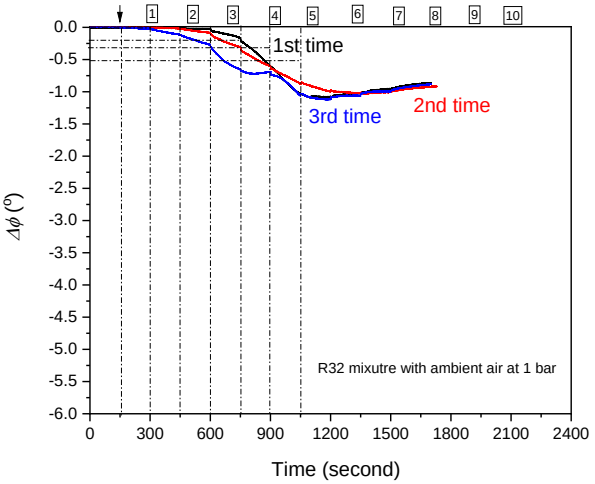

Figure 18. SAW sensor test result for the TBC4 coating on top of PVB layer in R32 ambient air mixture.

Based on these experiments, TBC4 deposited on a PVB layer through vacuum deposition showed better performance toward R32 compared to the TBC4/PVB mixture coated on the substrate with a drop coating. Therefore, the vacuum deposited TBC4 on PVB was tested in the R32 mixture with ambient air and the results were summarized in **Figure 18**. The relative humidity of the ambient air in the lab is about 35-40%. The test procedure and conditions are the same as previously described and the sensor measurement was repeated three times. The first sensor measurement was done after the fresh TBC4 deposition. The second senor measurement was repeated after the first measurement without any activation. The third sensor measurement was conducted after activation of the TBC4 at 120 ^{o}C for 15 minutes under vacuum. Compared to the R32 dry air mixture results shown in **Figure 17**, the phase shifts of the TBC4 film in R32 - ambient air mixture is smaller however the phase shift is reproducible after activating the sensor film for 15 min at 120 C under vacuum. Based on these results, we can conclude there is a clear response or phase shift where SAW coated with TBC4 when exposed to trace amounts of R32 in dry air as well as ambient air containing 35 – 40% of relative humidity. Our results further demonstrate the phase shift can be reproduced by activating the TBC4 film for 15 minutes at 120 C under vacuum. However, further experiments are needed to optimize the film thickness and optimization of phase shift with R32 in presence of other competing gases and vapors present in residential and commercial buildings.

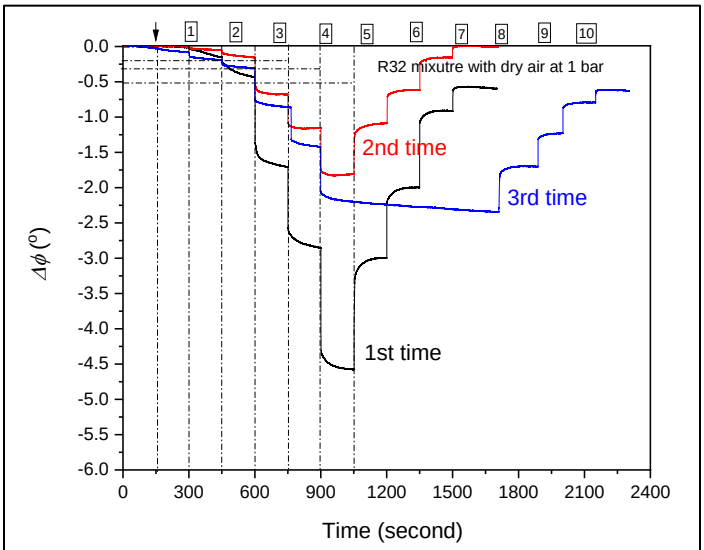

Figure 19. SAW sensor test result for the MIL-101/PVB mixture coating in R32 dry air mixture

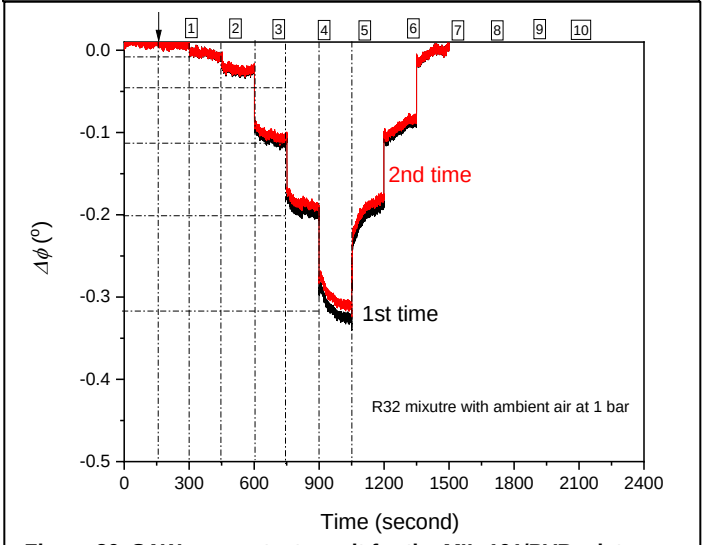

Figure 20. SAW sensor test result for the MIL-101/PVB mixture coating in R32 ambient air mixture.

Besides TBC4, MIL-101 was selected as another candidate for R32 sensing because of the high adsorption affinity toward R32. Like the TBC4/PVB mixture preparation, MIL-101/PVB (10%wt) methanol dispersion was prepared and coated to the SAW substrate through the drop coating method. The measurement procedure and conditions are the same and the results in the R32 dry air mixture are shown in **Figure 19**. The sensor performance was repeated three times that include i) sensor response or phase shift right after drop coating the MIL-101/PVB followed by flowing R32 with dry air mixture, ii) senor response after the first measurement without any activation and iii) The last experiment was conducted after activating the MIL-101 film for 15 min at 120 ^{o}C under vacuum. The phase shifts of MIL-101 in R32 dry air are much higher compared to those of the TBC4 (**Figure 16**), which is expected given higher adsorption capacity of MIL-101 towards R32 due to high surface area and pore volume. However, sensor response or phase shift was significantly reduced after subsequent tests and could not recover the phase shift even after activating the MIL-101 film. The same experiment was

repeated for the MIL-101/PVB in the R32 ambient air (humidity) mixture. The MIL-101/PVB layer was exposed to ambient air to saturate the film with water vapor adsorbed from ambient air and used without any further activation and the results are shown in **Figure 20**. Since the experiments were conducted after the sensor reached an equilibrium in ambient air, the phase shift was recorded by flowing the R32 over the MIL-101/PVB layer. As shown in Figure 21, a significant reduction in phase shift was observed compared to MIL-101/PVB layer activated at high temperature (**Figure 19**). The reduced phase shift was attributed to saturation of MIL-101/PVB film with water molecule when exposed to ambient air. The experiment was repeated twice and the phase shifts at 25,000 ppmv and 50,000 ppmv R32 in ambient air have a reproducible reading which demonstrates the selective R32 detection even in the presence of water vapor. Another possibility of reduced phase shift could be due to the lower glass transition temperature of PVB layer (~120 ^{o}C depending on the molecular weight). As a result, the PVB polymer may melt and penetrate inside the MIL-101. Therefore, the phase shifts for the MIL-101/PVB coating (**Figure 19**) are not large and need to be improved to get a better signal-to-noise ratio. Therefore, we selected another carbosiloxane polymer known as CSPH as shown in **Figure 21**. This CSPH polymer is a rubbery polymer that has no glass transition phase and behaves like liquid at room temperature. The same mixing and drop coating procedure were repeated as in the case of MIL-101/PVB to make MIL-101/CSPH coating. This mixture was coated on the AW SAW substrate and tested toward the R32 mixture with ambient air. The results are summarized in **Figure 21**. The measurement was repeated two times and no heating regeneration was included between the two measurements. Based on the plots, the results are reproducible. More importantly, the phase shifts are four times better than those in the case of MIL-101/PVB suggesting new CSPH polymer did help to eliminate any potential blockage of pores in the MIL-101. The long-term stability of the sensing coating may need further study which is not included in this stage of this project.

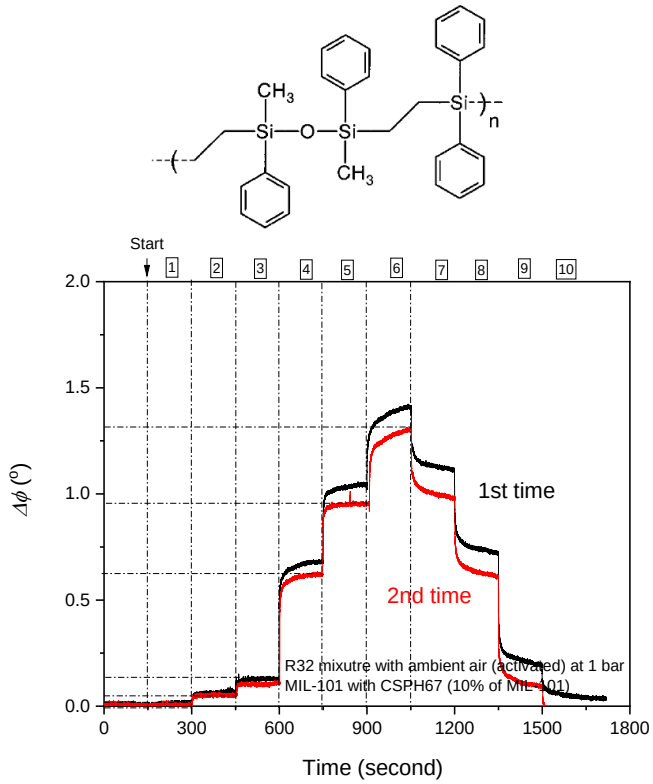

Figure 21. The repeat unit structure of the carbosiloxane polymer hydrogel (CSPH) and SAW sensor test result for the MIL-101/CSPH mixture coating in R32 ambient air mixture.

In conclusion, we successfully developed and demonstrate refrigerant leak detection using the SAW platform using a selective sorbent identified from the library of materials. Though the initial results are very promising, further experiments on SAW sensor needed to be performed that include i) optimization of the thin film thickness and robustness ii) SAW performance in presence of interfering gases and vapors including humidity, CO_2, toluene, ethyl acetate, acetone, isopropanol, ethanol (common contamination found in residential HVAC), iii) temperature drift on lab platform and engineered platform iv) sensor response time at 25% LFL and v) manufacturing methods to ensure strong mechanical coupling between the sorbent and piezoelectric substrate for optimal sensitivities and vi) impact of sorbent orientation on the SAW platform and so on before this technology can be commercialized.

4.0 References

1. Assawamartbunlue, K.; Brandemuehl, M. J., Refrigerant leakage detection and diagnosis for a distributed refrigeration system. Hvac&R Res 2006, 12 (3), 389-405.2.

2. Feng, W. Y.; Liu, L. H.; Zhang, X. P.; Zhao, X.; Huang, X. W.; Yu, C. H., Study on Leakage Detection Technology of Corrosive Acid Solution Based on Fiber Raman Temperature Measurement. Spectrosc Spect Anal 2020, 40 (11), 3425-3429.3.

3. Zheng, J.; Noh, H.; Chun, H. W.; Oh, B. M.; Lee, J.; Choi, S. K.; Kim, E.; Jung, D.; Lee, W. S.; Kim, J. H., Highly sensitive, selective, and rapid response colorimetric chemosensor for naked eye detection of hydrogen sulfide gas under versatile conditions: Solution, thin-film, and wearable fabric. Sensor Actuat B-Chem 2021, 341.4.

4. Schaef, H. T., V. A. Glezakou, A. T. Owen, S. Ramprasad, P. F. Martin, and B. P. McGrail, Surface Condensation of CO2 onto Kaolinite. Environ. Sci. Technol. Lett 2014, 1, 142.5.

5. Bender, F.; Skrypnik, A.; Voigt, A.; Marcoll, J.; Rapp, M., Selective detection of HFC and HCFC refrigerants using a surface acoustic wave sensor system. Anal Chem 2003, 75 (19), 5262-5266.6.

6. Rana, L.; Gupta, R.; Kshetrimayum, R.; Tomar, M.; Gupta, V., Fabrication of surface acoustic wave based wireless NO2 gas sensor. Surf Coat Tech 2018, 343, 89-92.7.

7. Gao, F.; Boussaid, F.; Xuan, W. P.; Tsui, C. Y.; Bermak, A., Dual Transduction Surface Acoustic Wave Gas Sensor for VOC Discrimination. Ieee Electr Device L 2018, 39 (12), 1920-1923.

8. Mcgill, R. A.; Grate, J. W.; Anderson, M. R., Surface and Interfacial Properties of Surface-Acoustic-Wave Gas Sensors. Acs Sym Ser 1994, 561, 280-294.9.

9. Dalgarno, S. J.; Thallapally, P. K.; Barbour, L. J.; Atwood, J. L., Engineering void space in organic van der Waals crystals: calixarenes lead the way. Chem Soc Rev 2007, 36 (2), 236-245.

10. Liu, J.; Thallapally, P. K.; McGrail, B. P.; Brown, D. R.; Liu, J., Progress in adsorption-based CO2 capture by metal-organic frameworks. Chem Soc Rev 2012, 41 (6), 2308-2322.

11. Motkuri, R. K.; Annapureddy, H. V. R.; Vijaykumar, M.; Schaef, H. T.; Martin, P. F.; McGrail, B. P.; Dang, L. X.; Krishna, R.; Thallapally, P. K., Fluorocarbon adsorption in hierarchical porous frameworks. Nature Communications 2014, 5.12.

12. Chen, L.; Reiss, P. S.; Chong, S. Y.; Holden, D.; Jelfs, K. E.; Hasell, T.; Little, M. A.; Kewley, A.; Briggs, M. E.; Stephenson, A.; Thomas, K. M.; Armstrong, J. A.; Bell, J.; Busto, J.; Noel, R.; Liu, J.; Strachan, D. M.; Thallapally, P. K.; Cooper, A. I., Separation of rare gases and chiral molecules by selective binding in porous organic cages. Nat Mater 2014, 13 (10), 954-960.

13. Thallapally, P. K.; McGrail, B. P.; Dalgarno, S. J.; Schaef, H. T.; Tian, J.; Atwood, J. L., Gas-induced transformation and expansion of a non-porous organic solid. Nat Mater 2008, 7 (2), 146-150.

14. Ferey, G.; Mellot-Draznieks, C.; Serre, C.; Millange, F.; Dutour, J.; Surble, S.; Margiolaki, I., A chromium terephthalate-based solid with unusually large pore volumes and surface area. Science 2005, 309 (5743), 2040-2042.

15. Ding M., Jiang H.-L. Improving water stability of metal–organic frameworks by a general surface hydrophobic polymerization. *CCS Chem.* 2020:2740–2748.

16. Yi B., Wong Y.L., Hou C., Zhang J., Xu Z., Yao X. Coordination-driven assembly of metal–organic framework coating for catalytically active superhydrophobic surface. *Adv. Mater. Interfaces.* 2021;8:2001202.

17. Use of quartz vibration for weighing thin films on a microbalance. *Z. Phys*., 155 (1959), pp. 206-222.

18. C. Steinem and A. Janshoff. Piezoelectric Sensors. Springer, 2007.

Pacific Northwest National Laboratory

902 Battelle Boulevard
P.O. Box 999
Richland, WA 99354
1-888-375-PNNL (7665)

www.pnnl.gov